Kronenberg, A.K., et al., 2020, Water loss during dynamic recrystallization of Moine thrust quartzites, northwest Scotland: Geology, v. 48, https://doi.org/10.1130/G47041.1

SUPPLEMENTAL INFORMATION

Water loss during dynamic recrystallization of Moine thrust quartzites, NW Scotland

Andreas K. Kronenberg, Kyle T. Ashley, Matthew K. Francsis, Caleb W. Holyoke III, Lynna Jezek, Johannes A. Kronenberg, Richard D. Law, Jay B. Thomas

The results and interpretations of this Geology paper are based on microstructural and IR absorption measurements of quartz grains in Cambrian quartzites collected from the footwall (Fig. S1) of the Moine thrust at the Stack of Glencoul, NW Scotland (Fig. 1). Supplemental information presented here includes the methods of microstructural and IR absorption measurements, tabulated results that appear in figures presented in the paper, and links to the archived digital data files.

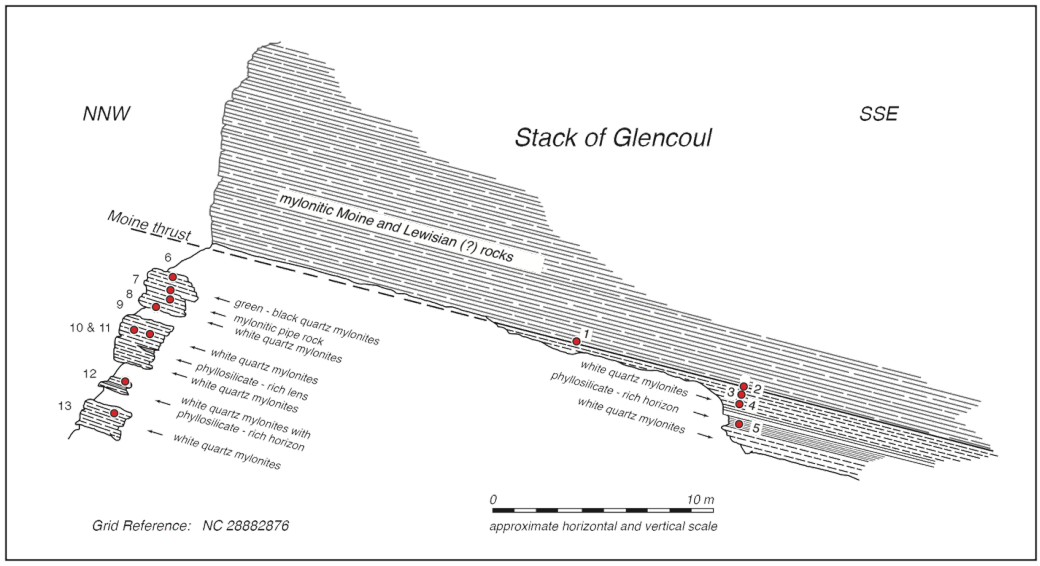

Figure S1. Sampling locations of mylonitic Cambrian quartzite samples SG-1 to SG-13 from the footwall of the Moine thrust at the Stack of Glencoul (after Law et al., 1986). Protolith Cambrian quartzite samples SG.14 and SG.15 were collected at 40 and 70 m beneath the thrust, respectively, and are separated from the overlying mylonitic quartzites along an unexposed thrust fault.

OPTICAL MICROSTRUCTURES

Deformation and dynamic recrystallization microstructures were observed in conventional (30 μm) thin sections of all samples SG-1 to SG-15, prepared perpendicular to foliation and parallel to lineation (the XZ plane) and imaged between crossed polarizers (Fig. 2). The extent of recrystallization of deformed quartz grains was quantified at the scale of whole sections (~20μm x 40 μm areas of observation) by applying a spatial mask over domains of recrystallized grains (or in cases of highly recrystallized samples, the original, deformed quartz grains) and determining the area fraction of recrystallized quartz using Image J software. These measurements are inferred to represent the volume % that has been dynamically recrystallized. Ultrathin, doubly polished sections (8-16 μm thickness) sections were prepared for selected samples (using methods of Kronenberg et al., 2017) to examine undulatory extinction, subgrain

boundaries, and recrystallized grains at high optical resolution, enhancing image brightness and contrast of the low optical retardation images using Adobe Photoshop (Fig. 2 A-C). Recrystallized grain sizes were measured in standard thickness sections (for $N > 400$ grains for selected sections) using the intercept method along traverses of several orientations to minimize sensitivity to grain shape. Chord lengths along the traverses were determined, and corrected to three-dimensional sizes (multiplying by a factor of 1.75) using methods described by Roth (2010) to find the arithmetic mean grain size. Standard deviations determined for each set of grain size measurements (s) reflect the distribution of measured grain sizes and the standard error of the mean ($s / \sqrt{N}$) reflects the uncertainty in the mean grain size determination. The correction factor converting chord length to three-dimensional grain size is appropriate when applying the theoretical piezometer of Twiss (1977) but uncorrected chord lengths should be used following methods of Stipp and Tullis (2003) when applying their experimental recrystallized grain size for quartz.

Microstructural measurements of recrystallized grains for samples SG-1 to SG-15 are compiled in Supplemental Table S1, including the structural distance of each sample below the Moine thrust, the fraction of quartz that has been recrystallized, the mean recrystallized quartz grain size, the standard deviation of grain size, the number of measurements of grain dimension, and the standard error of the mean. The proportions of the quartzites that are dynamically recrystallized decrease from ~97% just below the Moine thrust (0.005 m) to 17% (mostly at original quartz grain margins) at 70 m below the thrust. These measurements support the trend of % recrystallization with proximity to the Moine thrust reported by Weathers et al. (1979), although values for our samples are generally larger at a given structural distance (Figure 4A) than those of samples measured in the previous study. Some of our sections contain finely dispersed micas (identified in Table S1) and these sections tend to display lower proportions of recrystallized quartz grains than sections with few micas.

Supplemental Table S1. Microstructural measurements for recrystallized grains of quartzites beneath the Moine thrust, Stack of Glencoul, NW Scotland

Sample	Structural Distance below Thrust (m)	Recrystallized Grains				
		% Recrystallized	Mean Grain Size (μm)	Standard Deviation (μm)	N	Standard Error of Mean (μm)
SG-1*	0.005	97.46				
SG-2*	0.01	99.50				
SG-3	0.3	94.11	23.14	4.55	617	.18
SG-4	0.7	95.83	21.70	3.87	749	.14
SG-6	1.9	92.99	24.71	4.20	410	.21
SG-7*	2.5	62.74	19.15	5.59	757	.20
SG-8	2.9	76.67	22.90	4.16	710	.16
SG-9	3.55	74.17				
SG-10	4.6	72.16	21.25	3.76	668	.15
SG-11	4.6	66.06	20.05	3.07	803	.11
SG-12	7.3	47.93				
SG-13	8.5	58.84	20.39	3.31	692	.13
SG-14	40	20.31				
SG-15	70	17.35				

*domains of recrystallized quartz grains mixed with fine micas

Large penetrative strains are apparent from the large aspect ratio (ribbon) shapes of original detrital quartz grains (Christie, 1963) and lattice preferred orientations (LPO) indicate the onset of even larger shear strains (and large vorticities, *W*m) within recrystallized grains related to large shear displacements (within 0.2 m of the Moine thrust plane; Law et al., 1986, 2010). Thus, we interpret the trend of % recrystallization as a function of structural distance from the Moine thrust as a proxy for finite shear strains imposed during thrusting, which may exceed the relatively uniform, quantitative strains determined from grain shapes (Law et al., 2010).

Mean recrystallized grain sizes, as reported by Weathers et al. (1979), do not vary much (from 19 to 25 μm), even while their volume fraction and spatial occurrence at the grain scale vary significantly. These observations, combined with microstructural piezometers that relate mean recrystallized grain size to differential stress, independent of temperature and strain rate, (Twiss, 1977; Stipp and Tullis, 2003) lead us to concur with the conclusion of Weathers et al. (1979) that shear stresses during thrusting were nearly constant across the sampled traverse of the Moine thrust footwall, even while penetrative shear strains were localized. Shear stresses of 25-75 MPa were inferred by Weathers et al. (1979) using a number of microstructural piezometers. Preliminary applications of the Twiss (1977) and Stipp and Tullis (2003) piezometers to our grain size measurements fall within this range, with shear stresses of ~61 MPa based on the Twiss (1977) relationship and ~46 MPa based on the Stipp and Tullis (2003) piezometer, applying the Holyoke and Kronenberg (2010) correction (Francsis and Law, in preparation).

INFRARED ABSORPTION MEASUREMENTS

Doubly polished IR plates of uniform thickness (95-182 μm) were prepared perpendicular to foliation and parallel to lineation (the XY plane), and unpolarized IR spectra were measured using a Nicolet Magna 560 FTIR Spectrometer and NicPlan IR microscope, at a resolution of 4 cm^{-1} through a 100 μm square aperture (compiling 512 scans for each measurement) using methods described in Kronenberg et al. (2017). Integrated absorbances of OH stretching bands were determined, subtracting a linear background and separating OH absorbances of the broad band at 3400 cm^{-1} due to fluid inclusions in quartz grains and a sharper OH band at 3620 cm^{-1} due to mica inclusions. IR spectra represent results for individual quartz grains in all samples except for SG-1. Apertures were located well within larger quartz grains but this was more difficult to accomplish for smaller quartz porphyroclasts; as a result, spectra may sometimes include OH bands of water that is vicinal to or at grain boundaries. IR spectra for SG-1 include measurements for all larger, original quartz grains, but they also include results for polycrystalline domains of finely recrystallized quartz, selecting those domains with few intergranular white micas.

FTIR measurements for SG-1 to SG-15 are compiled in Supplemental Table S2, including integrated absorbances (in cm^{-2}) of the 3400 cm^{-1} and 3620 cm^{-1} OH bands due to fluid inclusions and mica inclusions, respectively, for 22-39 spectra of each sample. OH contents in molar ppm ($OH/10^6$ Si) due to fluid inclusions in quartz grains were determined using the calibration of Aines et al. (1984) for broad-band molecular water in quartz. Mean OH contents of quartz grains in SG-1 to SG-15, located at varying structural levels below the Moine thrust are listed in Supplemental Table S3, with standard deviations that represent variations in water contents of

quartz grains in a given sample and standard errors of mean OH content that represent uncertainties in the mean determination at a given structural level.

Supplemental Table S2. FTIR measurements of OH absorption bands of quartzites beneath the Moine thrust, Stack of Glencoul, NW Scotland

Sample	Structural Distance below Thrust (m)	OH Absorption Band Measurements				
		IR Plate thickness (μm)	Quartz Grain	Δ of 3400 cm^{-1} band (cm^{-2})	Δ of 3620 cm^{-1} band (cm^{-2})	OH Content* (ppm)
SG-1	0.005	95	1	2246	0	2358
			2	3967	0	4167
			3	3902	0	4097
			4	719	0	755
			5	1324	0	1390
			6	2258	19	2371
			7	368	42	386
			8	736	0	772
			9	671	369	705
			10	1155	0	1212
			11	1413	0	1483
			12	1763	0	1852
			13	1239	0	1301
			14	3227	0	3388
			15	920	627	966
			16	1165	0	1223
			17	878	0	922
			18	1352	0	1419
			19	848	0	891
			20	905	0	950
			21	612	0	642
			22	1201	151	1261
SG-7	2.5	106	1	1325	42	1391
			2	1520	1719	1596
			3	1364	66	1432
			5	2352	358	2470
			6	2317	495	2433
			7	1810	58	1901
			8	1937	12	2034
			9	778	50	817

Supplemental Table S2 (cont). FTIR measurements of OH absorption bands of quartzites beneath the Moine thrust, Stack of Glencoul, NW Scotland

Sample	Structural Distance below Thrust (m)	OH Absorption Band Measurements				
		IR Plate thickness (μm)	Quartz Grain	Δ of 3400 cm^{-1} band (cm^{-2})	Δ of 3620 cm^{-1} band (cm^{-2})	OH Content* (ppm)
SG-7	2.5	106	10	8030	302	8432
			14	356	162	374
			15	1570	235	1648
			16	2433	84	2555
			17	1203	25	1263
			18	1399	131	1469
			19	2051	610	2154
			20	1190	458	1249
			21	2414	1103	2535
			22	1353	677	1421
			23	2227	1711	2338
			24	2651	319	2784
			25	2220	1586	2331
			27	1882	238	1976
			28	3150	375	3308
			29	2261	33	2374
			30	2074	1078	2178
			31	3204	2000	3364
			32	2263	734	2376
			33	1454	383	1527
			34	7029	1600	7380
			35	2068	691	2171
			36	1942	759	2039
			37	614	28	645
			38	398	0	418
			40	1852	855	1945
			41	3115	509	3271
			42	1871	541	1965
			43	2075	1648	2179
SG-8	2.9	136	1	444	713	466
			2	1006	22	1056
			3	457	58	480
			4	1176	32	1235

Supplemental Table S2 (cont). FTIR measurements of OH absorption bands of quartzites beneath the Moine thrust, Stack of Glencoul, NW Scotland

Sample	Structural Distance below Thrust (m)	OH Absorption Band Measurements				
		IR Plate thickness (μm)	Quartz Grain	Δ of 3400 cm^{-1} band (cm^{-2})	Δ of 3620 cm^{-1} band (cm^{-2})	OH Content* (ppm)
SG-8	2.9	136	5	2269	432	2382
			6	766	319	804
			7	1089	162	1143
			8	1655	1174	1738
			9	121	107	127
			10	1091	74	1146
			11	1208	118	1268
			12	170	12	179
			13	404	94	424
			14	1369	61	1437
			15	880	115	924
			16	2554	1369	2682
			17	718	210	754
			18	1110	149	1165
			19	2648	495	2780
			20	2552	621	2680
			21	1971	88	2070
			22	1058	97	1111
			23	602	12	632
			24	1603	0	1683
			25	898	181	943
			26	967	469	1015
			27	1445	28	1517
			28	1649	137	1731
			29	1040	62	1092
			30	905	164	950
SG-10	4.6	120	1	1897	0	1992
			2	2376	238	2495
			3	1434	29	1506
			4	2393	46	2513
			5	2955	0	3103
			6	2332	0	2449

Supplemental Table S2 (cont). FTIR measurements of OH absorption bands of quartzites beneath the Moine thrust, Stack of Glencoul, NW Scotland

Sample	Structural Distance below Thrust (m)	OH Absorption Band Measurements				
		IR Plate thickness (μm)	Quartz Grain	Δ of 3400 cm^{-1} band (cm^{-2})	Δ of 3620 cm^{-1} band (cm^{-2})	OH Content* (ppm)
SG-10	4.6	120	8	1424	437	1495
			9	2775	0	2914
			11	2344	34	2461
			11B	3458	36	3631
			12	2030	22	2131
			13	3885	0	4079
			14	1448	0	1520
			17	2975	60	3124
			18	3432	95	3604
			19	2849	30	2991
			20	2346	17	2463
			21	2629	56	2760
			22	1255	111	1318
			23	2372	0	2491
			24	2113	0	2219
			26	4178	0	4387
			27	2405	0	2525
			28	2345	37	2462
			29	2091	236	2196
			30	982	61	1031
			31	2434	248	2556
			33	1835	77	1927
			35	2558	67	2686
			36	1930	149	2027
			37	2292	624	2407
			38	2634	24	2766
			39	2297	269	2412
			40	2066	111	2169
			41	1798	373	1888
			42	2118	339	2224
			44	1916	249	2012
			45	1539	162	1616
			46	2189	30	2298

Supplemental Table S2 (cont). FTIR measurements of OH absorption bands of quartzites beneath the Moine thrust, Stack of Glencoul, NW Scotland

Sample	Structural Distance below Thrust (m)	OH Absorption Band Measurements				
		IR Plate thickness (μm)	Quartz Grain	Δ of 3400 cm^{-1} band (cm^{-2})	Δ of 3620 cm^{-1} band (cm^{-2})	OH Content* (ppm)
SG-13	8.5	151	1	5616	43	5897
			2	4645	47	4877
			3	2776	0	2915
			4	2058	0	2161
			5	3098	0	3253
			6	1672	39	1756
			7	1765	33	1853
			8	2771	0	2910
			9	2200	0	2310
			10	2129	95	2235
			11	1895	0	1990
			12	1507	25	1582
			13	3849	88	4041
			14	1239	0	1301
			15	3019	0	3170
			16	2196	0	2306
			17	3211	43	3372
			18	2439	52	2561
			19	1534	12	1611
			20	2450	0	2573
			21	2721	0	2857
			22	1400	7	1470
			23	1920	95	2016
			24	1504	43	1579
			25	6022	0	6323
			26	1944	0	2041
			27	1710	25	1796
			28	1792	810	1882
			29	3386	61	3555
			30	1678	108	1762
SG-14	40	182	1	2994	82	3144
			2	2532	0	2659
			3	1286	428	1350

Supplemental Table S2 (cont). FTIR measurements of OH absorption bands of quartzites beneath the Moine thrust, Stack of Glencoul, NW Scotland

Sample	Structural Distance below Thrust (m)	OH Absorption Band Measurements				
		IR Plate thickness (μm)	Quartz Grain	Δ of 3400 cm^{-1} band (cm^{-2})	Δ of 3620 cm^{-1} band (cm^{-2})	OH Content* (ppm)
SG-14	40	182	4	1450	28	1523
			5	1557	0	1635
			6	2429	390	2550
			7	2146	0	2253
			8	674	0	708
			9	1462	0	1535
			10	865	0	908
			11	3172	2173	3331
			12	1634	1346	1716
			13	2022	0	2123
			14	1571	0	1650
			15	3502	137	3677
			16	277	0	291
			17	1601	253	1681
			18	1000	33	1050
			19	2187	0	2296
			20	1269	0	1332
			21	508	0	533
			22	1776	42	1865
			23	1665	225	1748
			24	3071	55	3225
SG-15	70	175	1	3566	17	3744
			2	2997	0	3147
			3	2435	0	2557
			4	5337	0	5604
			5	2875	0	3019
			6	3993	29	4193
			7	4029	0	4230
			8	1619	82	1700
			9	3001	12	3151
			10	2772	0	2911
			11	2067	0	2170
			12	2165	0	2273

Supplemental Table S2 (cont). FTIR measurements of OH absorption bands of quartzites beneath the Moine thrust, Stack of Glencoul, NW Scotland

Sample	Structural Distance below Thrust (m)	OH Absorption Band Measurements				
		IR Plate thickness (μm)	Quartz Grain	Δ of 3400 cm^{-1} band (cm^{-2})	Δ of 3620 cm^{-1} band (cm^{-2})	OH Content* (ppm)
SG-15	70	175	13	2285	0	2399
			14	3928	0	4124
			15	5291	0	5556
			16	4041	0	4243
			17	6579	0	6908
			18	6929	0	7275
			19	5056	0	5309
			20	5548	0	5825
			21	4388	0	4607
			22	3780	18	3969
			23	2657	14	2790
			24	2619	9	2750
			25	3672	0	3856
			26	4465	20	4688
			27	6069	16	6372
			28	4379	38	4598
			29	3092	0	3247
			30	3909	0	4104
			31	4027	23	4228
			32	4718	23	7954

*Using calibration of Aines et al. (1984) for molecular water in quartz (ppm in molar $OH/10^6Si$)

Supplemental Table S3. Mean OH contents of quartz grains in deformed quartzites beneath the Moine thrust, Stack of Glencoul, NW Scotland

Sample	Structural Distance below Thrust (m)	OH Contents			
		Mean OH in Quartz* (ppm)	Standard Deviation* (ppm)	N	Standard Error of Mean* (ppm)
SG-1	0.005	1569	1074	22	229
SG-7	2.5	2263	1550	37	255
SG-8	2.9	1254	713	30	130
SG-10	4.6	2432	707	39	113
SG-13	8.5	2665	1247	30	228
SG-14	40	1866	898	24	183
SG-15	70	4078	1397	32	247

*Using calibration of Aines et al. (1984) for molecular water in quartz
ppm in molar $OH/10^6Si$

DATA AVAILABILITY

Digital data files for IR absorbance spectra of Fig. 3, and the microstructural and IR absorption measurements of Supplemental Tables S1, S2, and S3 (some of which are displayed in Fig. 4) are available from the Texas Data Repository (https://data.tdl.org/). Data files (in csv format) and readme files (in txt format) can be downloaded either by entering "kronenberg" in the "Search" window of the Texas Data Repository page or visiting https://dataverse.tdl.org/dataverse.xhtml?alias=root&q=kronenberg.

REFERENCES CITED

Aines, R.D., Kirby, S.H., and Rossman, G.R., 1984, Hydrogen speciation in synthetic quartz: Phys. Chem. Minerals, v.11, p. 204-212, doi: 10.1007/BF00308135.

Christie, J.M., 1963, The Moine thrust zone in the Assynt region, northwest Scotland: University of California Publication Geological Science, v. 40, p. 345-440.

Francsis, M.K., and Law, R.D., in preparation, Piezometry and strain rate estimates of the Moine thrust, Stack of Glencoul, NW Scotland: intended for publication in J. Struct. Geol.

Holyoke, C. W., III and Kronenberg, A.K., 2010, Accurate differential stress measurement using the molten salt cell and solid salt assemblies in the Griggs rig with applications to strength, piezometers and rheology: Tectonophysics, v. 494, 17-31, doi:10.1016/j.tecto.2010.08.001.

Kronenberg, A.K., Hasnan, H.F.B., Holyoke III, C.W., Law, R.D., Liu, Z., and Thomas, J.B., 2017, Synchrotron FTIR imaging of OH in quartz mylonites: Solid Earth, v. 8, p. 1025-1045, doi: 10.5194/se-8-1025-2017.

Law, R.D., Casey, M., and Knipe, R.J., 1986, Kinematic and tectonic significance of microstructures and crystallographic fabrics within quartz mylonites from the Assynt and Eriboll regions of the Moine thrust zone, NW Scotland: Trans. Roy. Soc. Edinburgh: Earth Sciences, v. 77, p. 99-125.

Law, R.D., Mainprice, D., Casey, M., Lloyd, G.E., Knipe, R.J., Cook, B., and Thigpen, J.R., 2010, Moine thrust zone mylonites at the Stack of Glencoul: 1 - microstructures, strain and influence of recrystallization on quartz crystal fabric development: Geological Society, London, Special Publications, v. 335, p. 543-577, doi: 10.1144/SP335.23.

Roth, B.L., 2010, Flow Properties of Moine Thrust Zone Mylonites in Northern Assynt, NW Scotland: Masters Thesis, Virginia Tech, Blacksburg, VA, 111 p.

Stipp, M., and Tullis, J., 2003, The recrystallized grain size piezometer for quartz: Geophys. Res. Lett, v. 30, p. 3-1-3-5, doi:10.1029/2003GL018444.

Twiss, R.J., 1977, Theory and applicability of a recrystallized grain size paleopiezometer: Pure and Applied Geophysics, v. 115, p. 227-244, doi: 10.1007/BF01637105.

Weathers, M.S., Bird, J.M., Cooper, R.F., and Kohlstedt, D.L., 1979, Differential stress determined from deformation-induced microstructures of the Moine thrust zone: J. Geophys. Res., v. 84, p. 7495-7509, doi: 10.1029/JB084iB13p07495.